

## FOLDED TRIPLE-FREQUENCY QUASI-YAGI-TYPE ANTENNA WITH MODIFIED CPW-TO-CPS TRANSITION

Yang Ding<sup>\*</sup>, Yongchang Jiao, Biao Li, and Li Zhang

National Laboratory of Science and Technology on Antennas and Microwaves, Xidian University, Xi'an, Shaanxi 710071, China

**Abstract**—A novel side-feed quasi-Yagi type antenna capable of triple-frequency operation at about 1900, 2400 and 3600 MHz is presented in this paper. The antenna is composed of a folded quasi-Yagi element and a modified CPW-to-CPS transition. The proposed antenna can be mounted perpendicularly to the feed circuit board of an array antenna so that it offers a novel design with a free degree of feed point so as to save device space, and its folded quasi-Yagi element can result in a low profile to the system. The experimental results demonstrate that the proposed antenna can operate over three frequency bands, with  $-10$  dB reflection coefficient bandwidths of 200 MHz, 200 MHz, and 400 MHz at the central frequencies of 1.9, 2.4, and 3.6 GHz, respectively. Moreover, in the whole working bands, the antenna basically keeps the same radiation pattern and the gain is over 2.6 dBi.

### 1. INTRODUCTION

Nowadays, the explosive growth in the wireless communication is driving the increasing demand for antennas that integrate more than one communication system into a single compact module. Wireless applications such as 2G/3G/4G cellular phones, Global Positioning System, wireless local area network and Bluetooth have been developed at a fast pace during the past decade. The multiband planar antennas with directional pattern have attracted much attention because of their good features including low profile, light weight, low cost, ease of fabrication and high directivity. Printed monopole and dipole antennas etched on a dielectric substrate might be one of the simplest types

---

*Received 4 December 2012, Accepted 30 January 2013, Scheduled 31 January 2013*

\* Corresponding author: Yang Ding (dingyang4479@gmail.com).

of planar antennas and have been widely used for various wireless applications. The directional radiation characteristics are often achieved by antennas, whose dimensions are several wavelengths such as horn or reflector antennas, or arrays of antennas. Such dimensions are usually not a size-critical problem for outdoor applications or when working in a millimeter frequency band.

The planar quasi-Yagi antenna is widely used in wireless communication for its simple structure, easy to feed, low cost and high directivity [1–4]. Much significant effort has been devoted to designing quasi-Yagi antennas and various forms have been studied to improve the performance of quasi-Yagi antennas, such as the series-fed two bow-tie dipole array for enhancing the front-to-back ratio [5], the Sierpinski or Koch fractals shaped dipole elements for reduction in size [6–10], using resonators or parasitic elements for enhancing the gain and bandwidth, and various transitions for connecting to other components [11–13]. In [14], a quasi-Yagi antenna with arrow-shaped dipoles is proposed with the operating frequency from 490 to 798 MHz and gain between 3.8 and 5.7 dBi. A frequency and pattern reconfigurable Yagi antenna consisting of a PIN diode at the arms of the driver element with three switchable frequencies at 1.25 GHz, 1.85 GHz and 2.45 GHz is discussed in [15]. Most of them are fed by microstrip and working only in one or two operating bands. However, the uni-planar antennas are more beneficial than double-sided microstrip in terms of compactness and the integration capability with solid-state active and passive components.

In this paper, a new design for the uni-planar multiband quasi-Yagi antenna with a reduced size is developed. The proposed antenna consists of three quasi-Yagi elements of different lengths and three parasitic elements above the driver elements. The longest element is folded to reduce the antenna size. To match the input impedance of the antenna to the 50 ohm feed line, a modified integrated feed network consisting of a CPW line and CPS line is employed. The modified CPW-to-CPS transition can transform even-mode electrical field at the CPW line to odd mode electrical field at the CPS line and the side-feed structure is introduced. The effects of varying folded position of the quasi-Yagi elements on the antenna performances, such as the input reflection coefficient, are investigated. The proposed antenna, with  $-10$ -dB reflection coefficient operating band around 1.9, 2.4 and 3.6 GHz, covers several useful frequency bands including Personal Communication System (PCS, 1850–1990 MHz), wireless LAN (WLAN, 2400–2485 MHz), Industrial Science Medical (ISM, 2400–2500 MHz) band, TD-SCDMA Long-Term Evolution (TD-LTE, 2500–2690 MHz), and Worldwide Interoperability for Microwave

Access (WiMAX, 3400–3600 MHz). In addition, good directional radiation performance is achieved due to the characteristics of the Yagi antenna. The peak gains in the whole band are more than 2.6 dBi (from 2.6 dBi to 4.8 dBi).

## 2. ANTENNA DESIGN

The configuration of the proposed antenna is shown in Fig. 1. The antenna is fabricated on a FR4 substrate with chemical etching method and it has a thickness of 1.6 mm. The relative permittivity of the substrate is 4.4 and the dielectric loss tangent is 0.02. The overall size of the antenna is  $50 \times 50 \text{ mm}^2$ . The antenna is composed of a modified CPW-to-CPS transition, three driver dipole elements, arm 1, arm 2 and arm 3 with different length, and a simple ground plane as reflector element. Three parasitic elements are placed above the drivers. They can direct the wave propagation toward the endfire direction and can further improve the bandwidth of the antenna. Compared with the only one parasitic element in [16], three parasitic elements also can improve the inband gain. The driver dipole elements work as half-wave dipoles excited at different frequencies, while the nonexcited elements, longer or shorter than the excited element, act as reflectors or directors,

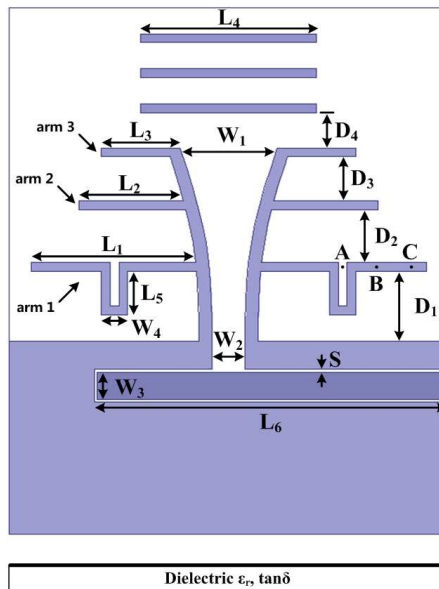


**Figure 1.** Structure of layout of the proposed quasi-Yagi-type antenna.

respectively. The lengths of driver dipole elements,  $L_1$ ,  $L_2$  and  $L_3$ , are approximately equal to  $\lambda_g/4$  ( $\lambda_g$  is the operating wavelength in the substrate) at their resonance frequencies. The distance between the dipole elements ( $D_2, D_3, D_4$ ) is chosen to be 0.1 to  $0.25\lambda_{g_{high}}$  ( $\lambda_{g_{high}}$  is the operating wavelength of the highest operating frequency in the substrate), according to principle of the Yagi antenna. The ground to the longest dipole element distance,  $D_1$ , can be chosen from 0.2 to  $0.35\lambda_{g_{high}}$  to improve the reflection coefficient. The final antenna parameters are fine-tuned and optimized by using the commercial electromagnetic solver High Frequency Structure Simulator (HFSS) and illustrated in Table 1.

In Fig. 1, a folded driver dipole element and other two shorter elements compose the basic quasi-Yagi element. Each of them can be simply model by a half-wave dipole connected to the different positions in feed line. When one of driver dipole elements works as a half-wave dipole, the other two elements behave as open-circuited parallel subs with infinite input impedance. As a result, one of the triple-frequency bands is created. Meanwhile, the elements as open-circuited parallel subs act as parasitic element with reflector or director functions, directing the main beam toward the endfire direction. In addition, the longest driver dipole element is folded to reduce the antenna size with a little effort on the reflection coefficient which will

**Table 1.** Optimized parameters (unit: mm).

Parameter	Value	Parameter	Value	Parameter	Value
$L_1$	18	$D_1$	8.2	$W_1$	11
$L_2$	13	$D_2$	6	$W_2$	3.7
$L_3$	11	$D_3$	5.8	$W_3$	3.1
$L_4$	20	$D_4$	4	$W_4$	3
$L_5$	6	$L_6$	40	$S$	0.3

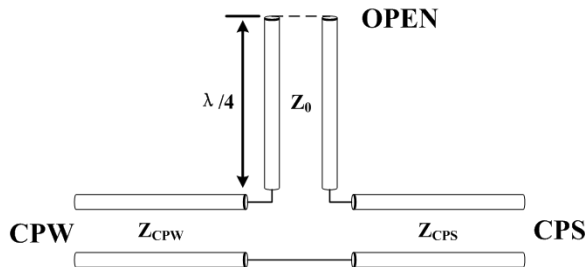


**Figure 2.** Simplified equivalent circuit for the CPW-to-CPS transition.

be explained in further detail below.

The feed network of the proposed antenna consists of the modified CPW-to-CPS transition. The original CPW-to-CPS transition is proposed in [16], the branch of which is used as a phase shifter. However this branch will cause the unequal current distribution on the feed line. The modified CPW-to-CPS transition changes the direction of the feed line, which has the same direction with the phase shifter in this paper. The current will be distributed symmetrically on the feed line and phase shifter. The simplified equivalent circuit of the CPW-to-CPS transition in Fig. 1 is shown in Fig. 2. It consists of a CPW feed line, an open-circuited quarter-wave CPW section in series and a CPS line. The open-circuited quarter-wave CPW section provides  $180^\circ$  phase delay from the CPW line and is capable of transforming an unbalanced input signal to a balance signal. The electric field lines and

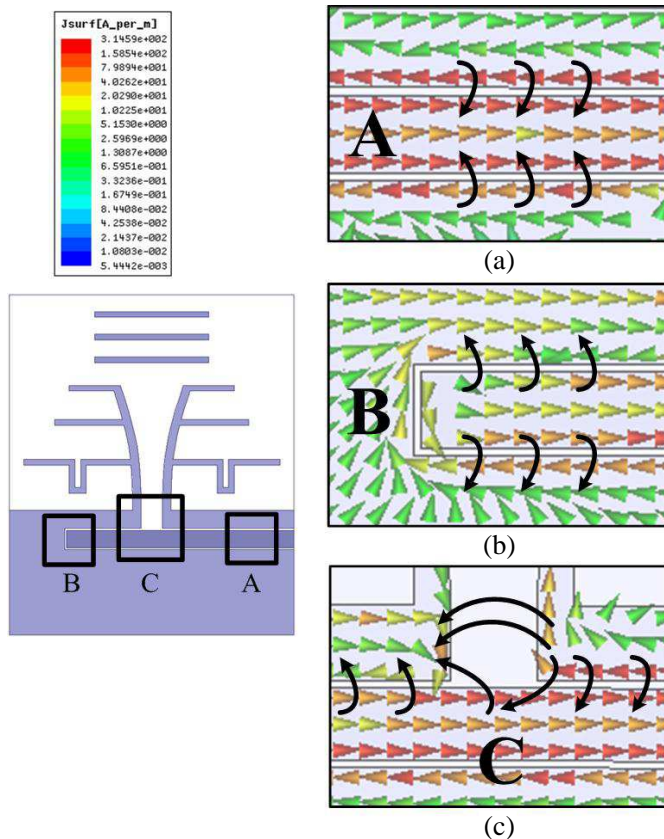


**Figure 3.** The electric field lines and current distribution on the CPW-to-CPS transition.

current distribution in various areas along the transition are described in Fig. 3. From these figures, it is seen that at area A shown in Fig. 3(a), the electric field and current distribution corresponds to the standard CPW line. With an open-circuited quarter-wave CPW section illustrated in Fig. 3(b), the electric field lines also correspond to the standard CPW line while the direction is changed through the phase shifter. At the reference area C, the electric field lines through the phase shifter and the normal one are assembled in the beginning of the CPS line. The electric field starts from the one side of the ground, then bridges to the strip, and eventually terminates at the other side of the ground, as formulated in Fig. 3(c). In this region, the electric field lines are partly across the strip and the field rotation is therefore initially constructed. Finally, as the strip vanishes, the electric field lines cross the other side of the CPS line as depicted in Fig. 3(c). With this process, the electromagnetic field realizes the rotation from CPW line to CPS line. A certain part of the modified CPS line whose width (from  $W_2$  to  $W_1$ ) increases along the line is applied. The  $W_1$  and  $W_2$  are optimized in order to improve the impedance to match the driver elements.

### 3. SIMULATED AND MEASURED RESULTS

The impedance characteristics of the proposed antenna are measured with the Agilent E8357A vector network analyzer. The measured and simulated reflection coefficients of the proposed antenna are presented in Fig. 4. Fig. 5 shows the simulated reflection coefficient for various folded part positions of longest driver element. The folded part connects to different locations on the driver dipole element, i.e.,

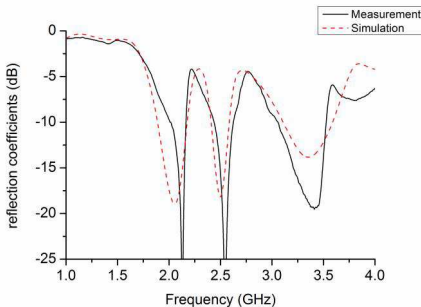


**Figure 4.** Measured and simulated reflection coefficients of the proposed antenna.

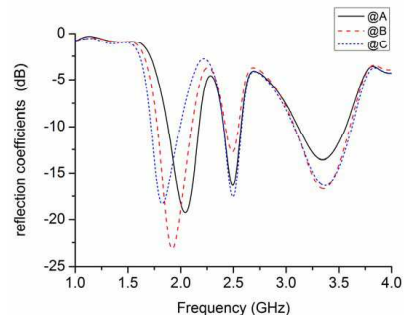


**Figure 5.** Simulated reflection coefficients for various folded part positions.

Points A, B, and C in Fig. 1. From the figure, it can be observed that the first resonant frequency is significantly decreased, while the bandwidth of the proposed antenna is unchanged. For the second and third band, the folded part influences the impedance characteristics slightly. The results indicate that changing the position of the folded part leads to a decrease of the third resonant frequency because the

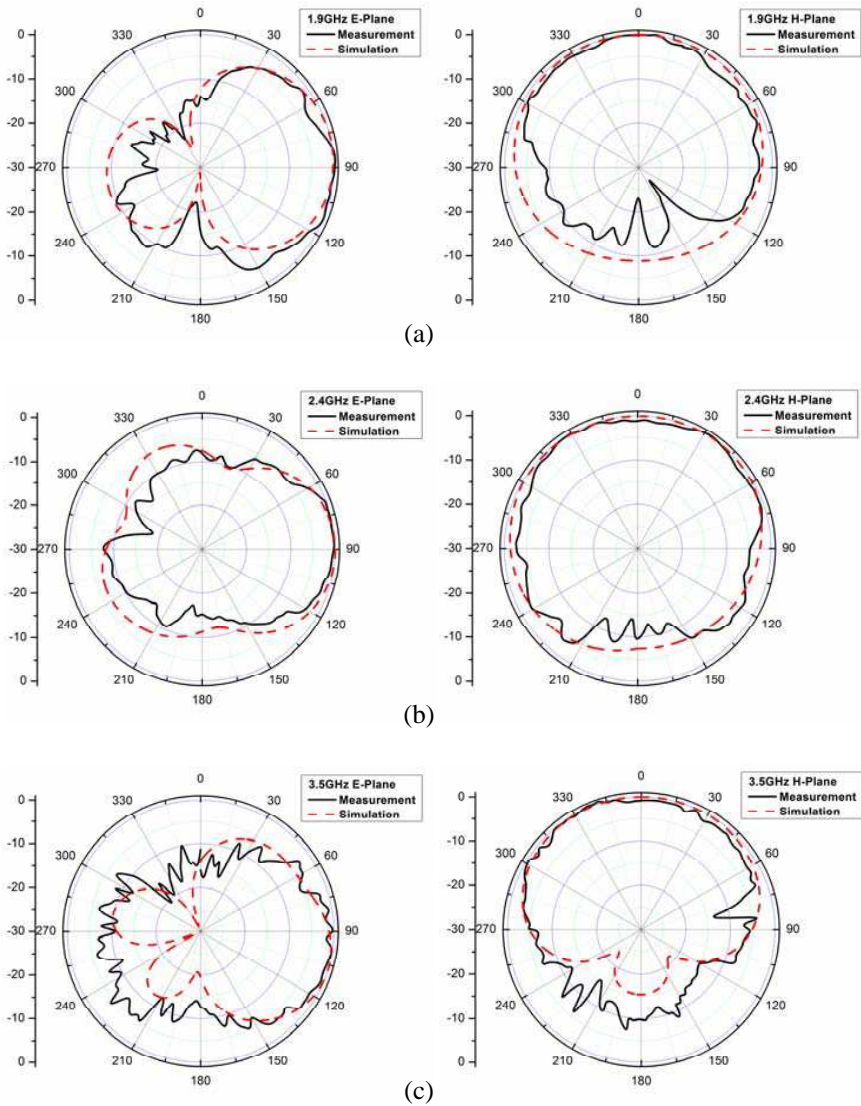


**Figure 6.** Measured and simulated radiation patterns at (a) 1.9, (b) 2.4, (c) 3.5 GHz, respectively.

current path is changed on the different part of the driver element.

In Fig. 6, the normalized measured and simulated radiation patterns for  $E$ - and  $H$ -planes for each band are illustrated. Referring to Fig. 6, the main beams are toward the endfire direction, and the front-to-back ratios are almost above 10 dB at the desired frequencies. The differences observed in the back radiation can be explained by the presence of the connector and coaxial cable for field testing. Except back lobes of the pattern, the agreement between the simulated and measured results is fairly good. Otherwise, the main direction of the pattern is slightly changed because the phase delay provided by the phase shifter is not identical through the three bands. The simulated and measured gain, bandwidth and radiation efficiency of the proposed antenna are shown in Table 2. Three measured section bandwidths according to  $-10$  dB reflection coefficient condition are 1.98–2.16 GHz, 2.43–2.63 GHz and 3.05–3.53 GHz, respectively. The measured gains are 2.6–4.8 dBi within operating bands.

**Table 2.** List of the measured (simulated) band characteristics.

Band	Bandwidth	Gain (dBi)	Radiation efficiency
1.9 GHz	1.98–2.16 GHz (1.9–2.1 GHz)	2.6–4.4 (3.8–5.0)	$\geq 67\%$
2.4 GHz	2.43–2.63 GHz (2.4–2.6 GHz)	3.5–3.7 (4.0–4.4)	$\geq 78\%$
3.6 GHz	3.05–3.53 GHz (3.2–3.6 GHz)	3.1–4.8 (4.1–4.9)	$\geq 70\%$

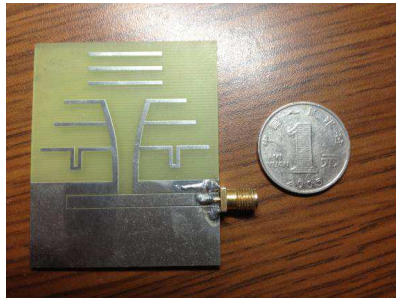


**Figure 7.** The fabricated prototype antenna.



#### 4. CONCLUSION

In this paper, a novel side-feed triple-frequency quasi-Yagi-type antenna has been proposed for mobile communication applications. A photograph of the antenna and its SMA connector is shown in Fig. 7. The antenna configuration and design methodology have been discussed. In the proposed antenna, three dipole elements of different lengths, serially connected through a modified CPS line, are used as Yagi elements for three operating bands and directional pattern. A modified integrated transition consisting of a CPW line and CPS line is employed to match the input impedance of the antenna to the 50ohm feed line. Simultaneously, the measured reflection coefficient and radiation patterns agree with the simulated ones. The structure of the proposed antenna not only is easy to be fabricated and modified for WLAN and other communication bands but also, because of the side-feed characteristic, is an element to form a larger array easily.

#### ACKNOWLEDGMENT

This work was supported in part by the National Natural Science Foundation of China (Grant No. 61201022), and in part by the Fundamental Research Funds for the Central Universities (Grant No. K50511020007).

#### REFERENCES

1. Sun, B.-H., S.-G. Zhou, Y.-F. Wei, and Q.-Z. Liu, "Modified two-element Yagi-Uda antenna with tunable beams," *Progress In Electromagnetics Research*, Vol. 100, 175–87, 2010.
2. Bemani, M. and S. Nikmeh, "A novel wide-band microstrip Yagi-Uda array antenna for WLAN applications," *Progress In Electromagnetics Research B*, Vol. 16, 389–406, 2009.
3. Bayderkhani, R. and H. R. Hassani, "Wideband and low sidelobe linear series FED Yagi-link antenna array," *Progress In Electromagnetics Research B*, Vol. 17, 153–167, 2009.
4. Chou, H. T., K. L. Hung, and C. Y. Chen, "Utilization of a Yagi antenna director array to synthesize a shaped radiation pattern for optimum coverage in wireless communications," *Journal of Electromagnetic Waves and Applications*, Vol. 23, No. 7, 851–861, 2009.
5. Yeo, J. and J.-I. Lee, "Series-fed two dipole array antenna using bow-tie elements with enhanced gain and front-to-back ratio,"

- Journal of Electromagnetic Waves and Applications*, Vol. 26, Nos. 11–12, 1641–1649, 2012.
6. Baliarda, C., J. Romeu, and A. Cardama, “The koch monopole: A small fractal antenna,” *IEEE Transactions on Antennas and Propagation*, Vol. 48, No. 11, 1773–1781, 2000.
  7. Teisbaek, H. B. and K. B. Jakobsen, “Koch-fractal Yagi-Uda antenna,” *Journal of Electromagnetic Waves and Applications*, Vol. 23, Nos. 2–3, 149–160, 2009.
  8. Chen, W., L. Jen, and S. Zhang, “Radiation pattern optimization for Yagi-Uda arrays of shaped dipole antennas,” *Electronics Letters*, Vol. 30, No. 16, 1264–1265, 1994.
  9. Gianvittorio, J. and Y. Rahmat-Samii, “Design, simulation, fabrication and measurement of a multiband fractal Yagi antenna,” *2003 IEEE Topical Conference on Wireless Communication Technology*, 265–266, 2003.
  10. Liu, S. and X. Zhang, “LCN for analysis of fractal Koch Yagi arrays,” *Asia-Pacific Conference Proceedings, Microwave Conference Proceedings, APMC 2005*, Vol. 4, 2005.
  11. Zheng, G., A. A. Kishk, A. B. Yakovlev, and A. W. Glisson, “Simplified feed for a modified printed Yagi antenna,” *Electronics Letters*, Vol. 40, No. 8, 464–465, 2004.
  12. Latif, S. I. and L. Shafai, “Gain enhancement of small microstrip antennas using multilayered laminated conductors,” University of Manitoba, 2007.
  13. Cheng, D. K., “Gain optimization for Yagi-Uda arrays,” *IEEE Antennas and Propagation Magazine*, Vol. 33, No. 3, 42–46, Jun. 1991.
  14. Mao, J. Y., Z. R. Li, Q. X. Guo, H. Zhang, X. Q. Zhang, X. F. Wu, and Y. Yang, “A wideband quasi-Yagi antenna with arrow-shaped dipoles for digital TV band applications,” *Journal of Electromagnetic Waves and Applications*, Vol. 26, No. 13, 1716–1723, 2012.
  15. Majid, H. A., M. K. A. Rahim, M. R. Hamid, and M. F. Ismail, “Frequency and pattern reconfigurable Yagi antenna,” *Journal of Electromagnetic Waves and Applications*, Vol. 26, Nos. 2–3, 379–389, 2012.
  16. Ding, Y., Y. C. Jiao, P. Fei, B. Li, and Q. T. Zhang, “Design of a multiband quasi-Yagi-type antenna with CPW-to-CPS transition,” *IEEE Antennas and Wireless Propag. Lett.*, Vol. 10, 1120–1123, 2011.